arXiv:1507.05851v1 [hep-ph] 21 Jul 2015

# Configuration mixing and effective baryon-baryon interactions

Xinmei Zhu[1], Hongxia Huang[1], Jialun Ping[1*], Fan Wang[2]
[1] *Department of Physics, Nanjing Normal University, Nanjing 210097, P.R. China and*
[2] *Department of Physics, Nanjing University, Nanjing 210093, P.R. China*

The effective baryon-baryon interactions is studied in the refined quark delocalization color screening model (QDCSM), in which the different quark clusterings are fully taken into account, instead of controlling by a variational delocalization parameter $\epsilon(s)$ between two 3-quark clusters. The symmetry bases are employed to do the calculation, all possible configurations for two quark clusters are considered. The results obtained are very similar to that of QDCSM. It is inferred that the delocalization parameter $\epsilon(s)$ used in QDCSM is an economic and effective way to describe the mixing of quarks between baryons.

PACS numbers: 12.39.Jh, 13.75.Cs, 14.40.Rt

## I. INTRODUCTION

Since the advent of quantum chromodynamics (QCD), the fundamental theory of strong interaction, it has been expected to calculate the properties of baryons and baryon-baryon (BB) interactions from QCD directly. However, the complexity of the non-perturbative character of QCD in the low energy region has hindered this attempt. Although the lattice QCD [1], Dyson-Schwinger equation approach [2], QCD sum rule [3], chiral perturbation theory [4] and other non-perturbative methods have made impressive progresses, the quark model approach is still the important method in hadron physics, especially for BB interaction and multiquark system. The quark model describes the experimental data of hadron properties and hadron-hadron interactions very well.

The naive quark model (Glashow-Isgur model [5]) successfully described the properties of baryons. However to extend it to BB interaction, refinements are necessary. One approach is to add the Goldstone-boson-exchange interaction to the Hamiltonian, it is developed to the chiral quark model [6]. After fine-tuning the model parameters, the model give a satisfactory description of BB interactions, where the $\sigma$-meson and other scalar mesons play an indispensable role. However, the $\sigma$-meson, as an $S$-wave resonance of $\pi\pi$ [7], cannot provide the expected intermediate-range attraction for nucleon-nucleon interaction [8]. In addition, how to realize the chiral partner in flavor $SU_3$ case is still a problem. The outstanding feature of the similarity between the nuclear force and molecular force can not have an explanation in this meson exchange model approach. The another approach is the quark delocalization color screening model (QDCSM) [9]. Two ingredients, quark delocalization and color screening, are introduced to enlarge the model space and modify the interactions of quark-pair in different quark clusters. This model is based on the same idea as Heitler and London's approach of hydrogen molecular structure. It explains the similarity between molecular force and nuclear force naturally. It also gives a good description of the BB interaction. Its predictions on $d^*$ dibaryon [10] had been confirmed by Celsius-WASA experiments [11], the prediction of $N\Omega$ dibaryon [12] is also supported by lattice QCD calculation [13]. In QDCSM, the color screening is used to lower the color confinement potential between two baryons and to facilitate the quark delocalization. The further studies show that the color screening phenomenology is an effective description of the hidden-color channels coupling [14]. The quark delocalization is realized by introducing a delocalization parameter $\epsilon(s)$, which is determined by the dynamics of the system,

$$\begin{aligned}
\psi_l(\mathbf{r}) &= \left(\phi_L(\mathbf{r}) + \epsilon\phi_R(\mathbf{r})\right)/N(\epsilon), \\
\psi_r(\mathbf{r}) &= \left(\phi_R(\mathbf{r}) + \epsilon\phi_L(\mathbf{r})\right)/N(\epsilon), \\
N(\epsilon) &= \sqrt{1+2\epsilon v+\epsilon^2}, \qquad v = \langle\phi_L|\phi_R\rangle,
\end{aligned}$$

Generally the un-delocalized single particle wavefunctions take the Gaussian form,

$$\begin{aligned}
|L\rangle \equiv \phi_L(\mathbf{r}) &= \left(\pi b^2\right)^{-\frac{3}{4}} e^{-\frac{1}{2b^2}(\mathbf{r}+\mathbf{S}/2)^2}, \\
|R\rangle \equiv \phi_R(\mathbf{r}) &= \left(\pi b^2\right)^{-\frac{3}{4}} e^{-\frac{1}{2b^2}(\mathbf{r}-\mathbf{S}/2)^2} \qquad (1)
\end{aligned}$$

In fact, the full delocalization can be realized by configuration mixing, i.e., taking all the configurations $|L^6\rangle, |L^5R\rangle, |L^4R^2\rangle, |L^3R^3\rangle, |L^2R^4\rangle, |LR^5\rangle$ and $|R^6\rangle$ into consideration for BB interaction, under the two cluster approximation. The mixing of the above seven configurations is determined by the dynamics of the system directly and no longer by one delocalization parameter $\epsilon$. In this way, the model space is larger than that of QDCSM. Fl. Stancu and L. Wilets had pointed that all the configuration are important in their studies of nucleon-nucleon interaction [15]. So it is interesting to study the BB interactions with the configuration mixing method and to check the validity and efficiency of delocalization method in QDCSM. For simplicity, the first version of QDCSM, where the interaction between quark pair consists of color confinement and one-gluon-exchange only, is employed in the present study.

---

[*] Corresponding author: jlping@njnu.edu.cn

TABLE I: The allowed $K$ for interesting sets of $\alpha$. The indices of the symmetries $[\nu], [\mu], [f]$ are: 1-[6]; 2-[51]; 3-[42]; 4-[33]; 5-[411]; 6-[321]; 7-[222]; 8-[3111]; 9-[2211].

| $\alpha$ | $K$ |
|---|---|
| 201 | 144 264 324 344 394 364 354 |
| 210 | 143 263 323 343 393 363 353 |
| 203 | 144 344 |
| $-400$ | 141 341 |
| $-1\frac{1}{2}2$ | 143 146 233 232 235 236 263 266 265 323 |
|  | 322 325 353 356 352 355 343 346 363 366 |
|  | 365 396 412 433 436 432 435 486 485 476 |

TABLE II: the allowed spatial symmetry for given $m, n$.

| $[\nu]$ | $L^6$ | $L^5R$ | $L^4R^2$ | $L^3R^3$ | $L^2R^4$ | $LR^5$ | $R^6$ |
|---|---|---|---|---|---|---|---|
| [6] | 1 | 1 | 1 | 1 | 1 | 1 | 1 |
| [51] | 0 | 1 | 1 | 1 | 1 | 1 | 0 |
| [42] | 0 | 0 | 1 | 1 | 1 | 0 | 0 |
| [33] | 0 | 0 | 0 | 1 | 0 | 0 | 0 |

TABLE III: The number of symmetry bases for interesting physical channels.

| YIJ | 201 | 210 | 203 | -400 | -1$\frac{1}{2}$2 |
|---|---|---|---|---|---|
| coupling channels | 27 | 27 | 10 | 10 | 96 |

This paper is organized as follows. In section II, the model Hamiltonian, the symmetry bases and the calculation method are described. The results are given in section IV and a summary is given in the last section.

## II. MODELS AND BASES

The model Hamiltonian is the same as that of QDCSM, which is described in detail in Ref.[9]. Here we only write down the Hamiltonian for 6-quark system,

$$\begin{aligned} H(6) &= \sum_{i=1}^{6}(m_i+\frac{\mathbf{p}_i^2}{2m_i})+\sum_{i<j=1}^{6} V_{ij}-T_c(6), \\ V_{ij} &= V_{ij}^c+V_{ij}^G, \\ V_{ij}^c &= -a_c\boldsymbol{\lambda}_i\cdot\boldsymbol{\lambda}_j \begin{cases} r_{ij}^2 & \text{if } i,j \text{ occur in the same baryon orbit,} \\ \frac{1-e^{-\mu r_{ij}^2}}{\mu} & \text{if } i,j \text{ occur in different baryon orbits.} \end{cases} \\ V_{ij}^G &= \alpha_s\frac{\boldsymbol{\lambda}_i\cdot\boldsymbol{\lambda}_j}{4}\left[\frac{1}{r_{ij}}-\frac{\pi}{2}\delta(\mathbf{r}_{ij})\left(\frac{1}{m_i^2}+\frac{1}{m_j^2}+\frac{4\boldsymbol{\sigma}_i\cdot\boldsymbol{\sigma}_j}{3m_im_j}\right)\right] \end{aligned} \quad (2)$$

To do the calculation, the symmetry bases are more convenient. The symmetry bases are the group-chain classification bases, which are defined as follows [16]

$$\Phi^{\alpha}_{Kmn}(q^6)=\left|\begin{array}{c}[\nu]L^mR^n \\ [\sigma]W[\mu]\beta[f]YIJM_IM_J\end{array}\right\rangle. \quad (3)$$

where $\alpha=(YIJ)$ are the strong interaction conserved quantum numbers: strangeness, isospin and spin. $K$ denotes the intermediate quantum numbers, $[\nu], [\mu], [f]$. $[\nu], [\mu], [\sigma], [f]$ represent the symmetry of orbital, spin-flavor $SU(6)$, $SU(3)$ color and flavor. $[\sigma]=[222]$ is fixed due to the color singlet requirement. For some interesting sets of quantum numbers $\alpha$, the allowed intermediate quantum numbers $K$ are listed in Table I. Table II presents the allowed spatial symmetries $[\nu]$ for given $m,n$. The number of symmetry bases for given $\alpha$ can be obtained from the combination of the allowed $K$ and $m,n$, which is given in Table III.

For illustration, two bases of the ten bases for channel $\alpha=(YIJ)=203$ are shown below,

$$\begin{aligned} \Phi^{(203)}_{144\ 51}(q^6) &= \left|\begin{array}{c}[6]L^5R^1 \\ [222]1[33]1[33]20303\end{array}\right\rangle, \\ \Phi^{(203)}_{344\ 24}(q^6) &= \left|\begin{array}{c}[42]L^2R^4 \\ [222]1[33]1[33]20303\end{array}\right\rangle. \end{aligned}$$

where $M_I, M_J$ take their maximum values, the eigenenergies are independent of $M_I, M_J$.

To study the BB interaction, the Schrödinger equation for 6-quark system has to be solved,

$$H(6)\Psi^{\alpha}(q^6)=E^{\alpha}\Psi^{\alpha}(q^6), \quad (4)$$

where the eigen wavefunction $\Psi^{\alpha}$ is the linear combination of $\Phi^{\alpha}_{Kmn}(q^6)$ under the cluster approximation,

$$\Psi^{\alpha}(q^6)=\sum_{Kmn}c^{\alpha}_{Kmn}\Phi^{\alpha}_{Kmn}(q^6). \quad (5)$$

By using Eq.(5), Eq.(4) becomes

$$\sum_{k'}\left[\langle\Phi^{\alpha}_{k'}|H(6)|\Phi^{\alpha}_{k}\rangle-E^{\alpha}\langle\Phi^{\alpha}_{k'}|\Phi^{\alpha}_{k}\rangle\right]c^{\alpha}_{k}(q^6)=0, \quad (6)$$

where $k$ stands for $Kmn$. The eigen energy of the system can be obtained by solving the generalized eigen equation. the calculation of the 6-quark Hamiltonian matrix elements on the symmetry basis is performed by the well known fractional parentage expansion technique [16].

$$\begin{aligned} \langle\Phi^{\alpha}_{k}|H|\Phi^{\alpha}_{k'}\rangle &= \sum\binom{6}{2}\langle\Phi^{\alpha}_{k}|\alpha_1k_1,\alpha_2k_2\rangle\langle\alpha'_1k'_1,\alpha'_2k'_2|\Phi^{\alpha}_{k'}\rangle \\ &\quad \langle\alpha_1k_1|\alpha'_1k'_1\rangle\langle\alpha_2k_2|H_{56}|\alpha'_2k'_2\rangle. \end{aligned} \quad (7)$$

where $\langle\alpha_1k_1|\alpha'_1k'_1\rangle$ is the four quark overlap. $\langle\alpha_2k_2|H_{56}|\alpha'_2k'_2\rangle$ is the two body matrix element and $H_{56}$ represents the two-body operator for the last pair. $\langle\Phi^{\alpha}_{k}|\alpha_1k_1,\alpha_2k_2\rangle$ and $\langle\alpha'_1k'_1,\alpha'_2k'_2|\Phi^{\alpha}_{k'}\rangle$ are the total coefficients of fractional parentage. All the needed coefficients can be obtained from the Chen's book [17].

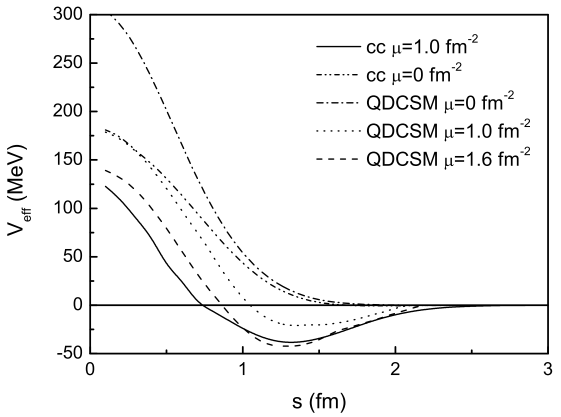

FIG. 1: The effective potentials for $NN$ with $YIJ = 201$. 'cc' stands for configuration mixing calculation.

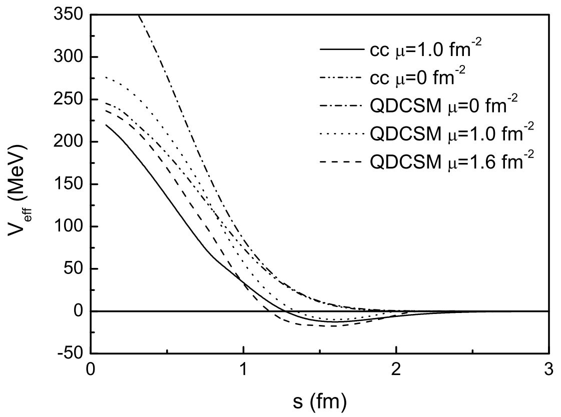

FIG. 2: The same as Fig. 1 for $NN$ with $YIJ = 210$.

TABLE IV: The parameters used in the calculations.

| $m$(MeV) | $m_s$(MeV) | $b$(fm) | $\alpha_s$ | $a_c$(MeV·fm$^{-2}$) | $\mu$(fm$^{-2}$) |
|---|---|---|---|---|---|
| 313 | 633.76 | 0.603 | 1.54 | 25.13 | 0 or 1.0 |

## III. RESULTS

The effective potentials between two baryons in the $u, d, s$ 3-flavor world are calculated in the framework of the refined QDCSM. The effective potential is defined as

$$V_e = E_6(s) - E_6(S = \infty) \tag{8}$$

where $E_6(s)$ is the eigen-energy of 6-quark system with separation $s$. To save space, only the results of several interesting states are given below. The needed model parameters are all taken from QDCSM, which is listed in Table IV.

Before presenting the results, we discuss the problem of numerical calculation first. When the separation between two clusters is very small, the difference between $L$ and $R$ goes to vanishing, the set of bases of the system will be over complete. To remove the spurious bases, the eigen method is used. First the overlap matrix of the system is diagonized, the eigenvectors corresponding to zero eigenvalues are dropped. Then the Hamiltonian matrix is reproduced on the remained eigenvectors of overlap matrix with non-zero eigenvalues. At last the new Hamiltonian matrix is diagonized to get the eigen-energy of the system.

Another problem needs to mention is associated with two configurations $L^6$ and $R^6$. Physically, these two configurations are the same, and the energies of these two configurations do not change with the separation between two clusters. In fact, these two configurations almost do not contribute to the effective potentials.

Figs. 1-5 give the effective potentials between two baryons with quantum numbers $YIJ$ = 201, 210, 203, $-1\frac{1}{2}2, -400$. For comparison, the results for $\mu = 0$ fm$^{-2}$ (without color screening) and the results of QDCSM are also shown in these figures. Clearly, the effective potentials go to zero when the separation becomes large (e.g., $s = 3$ fm), due to characteristic of confinement and one-gluon-exchange potentials and the Gaussians used as the wavefunctions of single-particle. All figures also show the differences between the present approach and QCDSM gradually disappear when the separation becomes large, because the color confinement pushes the energies of the hidden color configurations, $[6]R^5L^1$, $[6]R^4L^2$, $[6]R^2L^4$, $[6]R^1L^5$, $[42]R^4L^2$, $[42]R^2L^4$, higher.

Fig. 1 shows the effective potentials between two nucleons with quantum numbers $YIJ = 201$. If there is no color screening effect, i.e., $\mu = 0$ fm$^{-2}$, then the intermediate range attraction is missing both in present work and in QDCSM, and QDCSM have a larger repulsive core. Taking into account of the color screening effect, the intermediate range attraction is obtained in both approaches. The attraction in QDCSM is about half of that in the present approach. This is reasonable, because the variational space in the present approach is larger than that in QDCSM. Even though all the configurations, $|L^6\rangle, |L^5R\rangle, |L^4R^2\rangle, |L^3R^3\rangle, |L^2R^4\rangle, |LR^5\rangle$ and $|R^6\rangle$ are included in QDCSM, the percentages of different configurations are controlled by one variational parameter $\epsilon$, which is determined by system dynamics. Whereas in the refined QDCSM the dynamics of system fix the configuration mixing with 7 coefficients (see Table V). By increase the color screening parameter, e.g., $\mu = 1.6$ fm$^{-2}$, QDCSM can produce almost the same effective potentials as the present approach.

The effective potentials for $NN$ with $YIJ = 210$ are shown in Fig. 2. The results of comparison between two approaches are similar to that of $NN$ with $YIJ = 201$.

For $YIJ = 203$ $\Delta$-$\Delta$ channel, attractions appear in all cases (see Fig. 3). The color screening introduces much stronger attraction. With the same color screening parameter, the present approach give a little stronger

TABLE V: The relative probabilities of different configurations in the states for $YIJ = 203$ with $\mu = 1.0$ fm$^{-2}$.

| | $s = 4$ fm | | $s = 2.6$ fm | | $s = 2$ fm | | $s = 1.1$ fm | | $s = 0.5$ fm | |
|---|---|---|---|---|---|---|---|---|---|---|
| | This work | QDCSM | This work | QDCSM | This work | QDCSM | This work | QDCSM | This work | QDCSM |
| $[6]R^6$ | 0.00 | 0.00 | 0.33 | 0.00 | 0.27 | 0.01 | 0.00 | 0.02 | 0.00 | 0.00 |
| $[6]R^5L^1$ | 0.00 | 0.00 | 0.01 | 0.00 | 0.47 | 0.14 | 0.00 | 0.19 | 0.05 | 0.11 |
| $[6]R^4L^2$ | 0.00 | 0.00 | 0.04 | 0.11 | 0.74 | 0.61 | 0.25 | 0.67 | 0.08 | 0.59 |
| $[6]R^3L^3$ | 1.00 | 1.00 | 1.00 | 1.00 | 1.00 | 1.00 | 1.00 | 1.00 | 1.00 | 1.00 |
| $[6]R^2L^4$ | 0.00 | 0.00 | 0.04 | 0.11 | 0.74 | 0.61 | 0.25 | 0.67 | 0.08 | 0.59 |
| $[6]R^1L^5$ | 0.00 | 0.00 | 0.01 | 0.00 | 0.47 | 0.14 | 0.00 | 0.19 | 0.05 | 0.11 |
| $[6]L^6$ | 0.00 | 0.00 | 0.33 | 0.00 | 0.27 | 0.01 | 0.00 | 0.02 | 0.00 | 0.00 |
| $[42]R^4L^2$ | 0.00 | 0.00 | 0.02 | 0.07 | 0.12 | 0.09 | 0.01 | 0.00 | 0.01 | 0.00 |
| $[42]R^3L^3$ | 4.00 | 4.00 | 3.79 | 3.29 | 0.61 | 0.36 | 0.01 | 0.00 | 0.00 | 0.00 |
| $[42]R^2L^4$ | 0.00 | 0.00 | 0.02 | 0.08 | 0.12 | 0.09 | 0.01 | 0.00 | 0.01 | 0.00 |

attraction than QDCSM in the short-range part. Increasing the color screening parameter in QDCSM, the curve will move downward, getting close to the results of the present approach. Due to the strong attraction, the bound state with respect to two Δ's can be formed. Taking into account the four-body decay channel, $NN\pi\pi$, a resonance appears in this channel, which was observed in WASA-at-COSY experiments [11]. To show the reason for the similarity between two approaches in detail, the relative probabilities of different configurations in the given states, the ratios of probability of a configuration to the configuration $[6]R^3L^3$, are tabulated in Table V. Due to the symmetry between left and right Gaussians, the probabilities of the configuration $[\nu]R^mL^n$ in the states are identical to that of $[\nu]R^nL^m$. From this table, we can see that the same physical states are obtained in the two approaches when the separation is large enough ($s = 4$ fm). With the decreasing of the separation, the differences between the two approaches appear gradually. However, the main configurations in the states are kept the same, $[6]R^3L^3$, $[42]R^3L^3$ and $[6]R^4L^2$, $[6]R^2L^4$. Even as the separation becomes very small, the superficial large difference between two approaches will be reduced remarkably because of the large overlap among the configurations $[6]R^mL^n$ with different $m, n$, due to the fact that there is no much difference between the right and left gaussians.

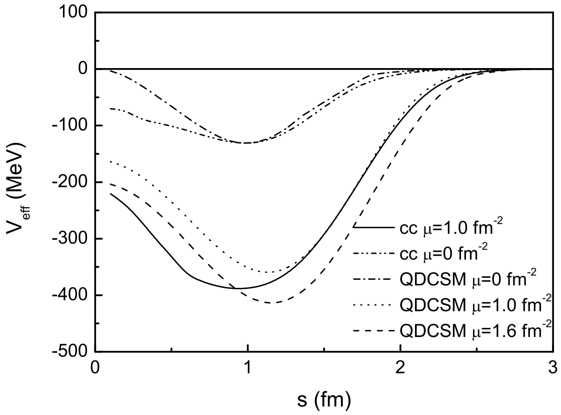

FIG. 3: The same as Fig. 1 for $NN$ with $YIJ = 203$.

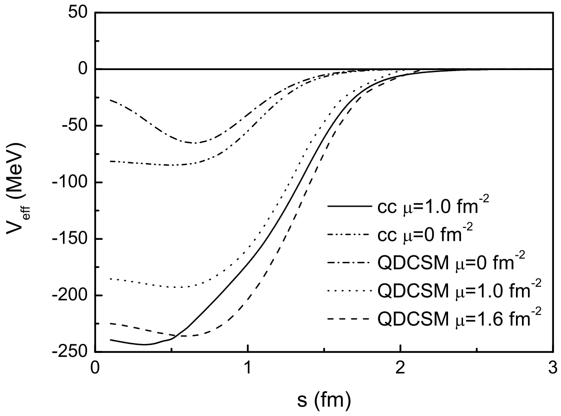

FIG. 4: The same as Fig. 1 for $N\Omega$ with $YIJ = -1\frac{1}{2}2$.

The effective potentials of $N\Omega$ with $YIJ = -1\frac{1}{2}2$ are given in Fig. 4. Again, attractions appear in all cases, the color screening increases the attraction about 100 MeV at the short-range part. A resonance is expected to be formed in this channel because of the deep attraction. The dynamical calculation of quark model and the lattice QCD calculation supported this result.

Di-Ω as a possible dibaryon candidate was predicted in 1990 [18] and also proposed by Li *et al.* in 2001 [19]. From Fig. 5, we can see that the effective potential between two Ω's has a mild attraction in QDCSM with color screening $\mu = 1$ fm$^{-2}$. However, a rather strong attraction in the short-range part is obtained in the present approach with the same $\mu$. Taking into account the fact that the two Ω's can form a weak bound state in QDCSM, it is expected that the ΩΩ with $YIJ = 400$ is a good dibaryon candidate.

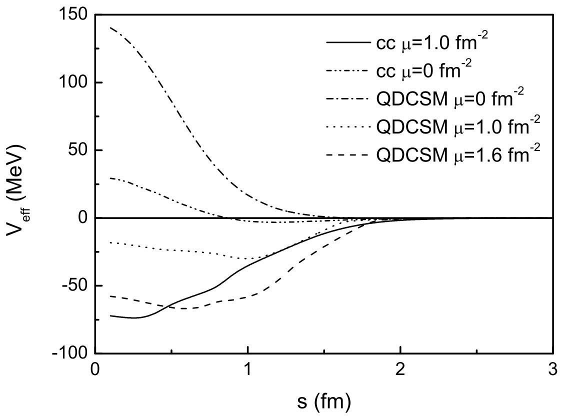

FIG. 5: The same as Fig. 1 for $\Omega\Omega$ with $YIJ = -400$.

## IV. SUMMARY

By enlarging the model space, i.e., taking into account of all possible configurations under the constraint of two clusters, the effective potentials are obtained for the BB systems. In most cases, the potentials obtained in the present approach are similar to the ones obtained in QDCSM, except at the short-range part, where lower potentials obtained in this approach. The results show the validity of the delocalization in QDCSM.

From the results for NN channels, the configuration mixing themselves does not lead to the intermediate-range attraction unless the color screening effect is introduced. The possible dibaryon candidates based on the present results are similar to that of the previous work [16]. Maybe $\Omega\Omega$ will have a little large binding energy in the present approach. To obtain more reliable results for dibaryons, the dynamical calculation is indispensable, which is in progress.

### Acknowledgments

This work is supported partly by the National Science Foundation of China under Contract Nos. 11175088, 11035006, 11265017

---

[1] S. Aoki, PoS (Hadron 2013) 020 (arXive:1402.3059) and references therein.

[2] H. L. L. Roberts, L. Chang, I. C. Cloet and C. D. Roberts, Few Body Syst. **51**, 1 (2011) and references therein.

[3] L. J. Reinders, H. Rubinstein and S. Yazaki, Phys. Rep. 127, 1, (1985); H. X. Chen, A. Hosaka and S. L. Zhu, Mod. Phys. Lett. A23, 2234 (2008); H. X. Chen, E. L. Cui, W. Chen, T. G. Steele and S. L. Zhu, arXiv:1410.0394.

[4] S. Scherer, Adv. Nucl. Phys. 27, 277 (2003); V. Bernard and U. Meisner, Ann. Rev. Nucl. Part. Sci. 57, 33 (2007).

[5] N. Isgur and G. Karl, Phys. Rev. D **18**, 4187 (1978); **19**, 2653 (1979); **20**, 1191 (1979).

[6] Y. Fujiwara, C. Nakamoto and Y. Suzuki, Phys. Rev. C **54**, 2180 (1996); Z. Y. Zhang, Y. W. Yu, P. N. Shen *et al.*, Nucl. Phys. **625**, 59 (1997); A. Valcarce, H. Garcilazo, F. Fernandez and P. Gonzalez, Rep. Prog. Phys. **68**, 965 (2005) and references therein.

[7] M. Ablikim *et al.* (BES Collaboration), Phys. Lett. B **598**, 149 (2004).

[8] N. Kaiser, S. Grestendorfer, and W. Weise, Nucl. Phys. A **637**, 395 (1998); E. Oset, H. Toki, M. Mizobe, and T. T. Takahashi, Prog. Theor. Phys. **103**, 351 (2000); M. M. Kaskulov and H. Clement, Phys. Rev. C **70**, 014002 (2004).

[9] F. Wang, G. H. Wu, L. J. Teng, and T. Goldman, Phys. Rev. Lett. 69, 2901 (1992); G. Wu, L. Teng, J. L. Ping, F. Wang, and T. Goldman, Phys. Rev. C 53, 1161 (1996); J. L. Ping, F. Wang, and T. Goldman, Nucl. Phys. A657, 95 (1999); G. H. Wu, J. L. Ping, L. J. Teng, F. Wang, and T. Goldman, Nucl. Phys. A673, 279 (2000); H. R. Pang, J. L. Ping, F. Wang, and T. Goldman, Phys. Rev. C 65, 014003 (2001).

[10] T. Goldman, K. Maltman, G. J. Stephenson, K. E. Schmidt, and F. Wang, Phys. Rev. C **39**, 1889 (1989); J. L. Ping, F. Wang and T. Goldman, Nucl. Phys. A **688**, 871 (2001); J. L. Ping, H. R. Pang, F. Wang and T. Goldman, Phys. Rev. C **65**, 044003 (2002); J. L. Ping, H. X. Huang, H. R. Pang, F. Wang, and C. W. Wong, Phys. Rev. C **79**, 024001 (2009).

[11] M. Bashkanov *et al.* (CELSIUS-WASA Collaboration), Phys. Rev. Lett. **102**, 052301 (2009); P. Adlarson *et al.* (WASA-at-COSY Collaboration), Phys. Rev. Lett. **106**, 242302 (2011); P. Adlarson *et al.* (WASA-at-COSY Collaboration), Phys. Lett. B **721**, 229 (2013); P. Adlarson *et al.* (WASA-at-COSY Collaboration), Phys. Rev. Lett. **112**, 202301 (2014).

[12] T. Goldman, K. Maltman, G. J. Stephenson, K. E. Schmidt and F. Wang, Phys. Rev. Lett. **59**, 627 (1987); H. R. Pang, J. L. Ping, F. Wang, T. Goldman and E. G. Zhao, Phys. Rev. C **69**, 065207 (2004).

[13] F. Etminan, H. Nemura, S. Aoki, *et al.* [HAL QCD Collaboration], Nucl. Phys. A **928**, 89 (2014).

[14] H.X. Huang, P. Xu, J. L. Ping and F. Wang, Phys. Rev. C **84**, 064001 (2011).

[15] Fl. Stancu and L. Wilets, Phys. Rev. C **36**, 726 (1987); **38**, 1145 (1988); **40**, 1901 (1989).

[16] F. Wang, J. L. Ping and T. Goldman, Phys. Rev. C **51**, 1648 (1995); 3346 (1995).

[17] J.Q. Chen *et al.*, *Tables of the Clebsh-Gordan, Racah and Subduction Coefficients of* $SU(n)$ *Groups,* 1987 (World Scientific, Singapore); *Tables of the* $SU(mn) \supset SU(m) \times SU(n)$ *Coefficients of Fractional Parentage,* 1991 (World Scientific, Singapore).

[18] V. B. Kopeliovich, B. Schwesinger, and B. E. Stern, Phys. Lett. B **242**, 145 (1990).

[19] Q. B. Li, P. N. Shen, Z. Y. Zhang, and Y. W. Yu, Nucl.

Phys. A **683**, 487 (2001)